

# Design Capacitive Pressure Sensor (MEMS) with High Sensitivity and Linearity for Biomedical Application

Mokhalad Alghairi\*<sup>1</sup>, Emad Hmood Salman<sup>2</sup>, Basim Abdul Kareem Farhan<sup>1</sup>, Waleed Algriree<sup>3</sup>, Hussein Mohammed Ridha<sup>4</sup>, Saad Mutashar<sup>5</sup>, Nasri Sulaiman<sup>6</sup>

<sup>1</sup>Department of Computer Techniques Engineering, Imam Alkadhim University College, Baghdad, Iraq

<sup>2</sup>Department of Communications Engineering, College of Engineering, University of Diyala, Diyala, Iraq

<sup>3</sup>Department of Medical Instrumentation Techniques Engineering, Dijlah University College, Baghdad, Iraq

<sup>4</sup>Department of computer Engineering, Mustansiriyah University, Baghdad, Iraq

<sup>5</sup>Department of Medical Instrumentation Techniques Engineering Department, Al-Mustaqbal University, Hillah, Iraq

<sup>6</sup>Department of Electrical and Electronic Engineering, Faculty of Engineering, Universiti Putra Malaysia, Serdang 43400, Selangor, Malaysia

Correspondance

\*Mokhalad Alghairi

Department of Computer Techniques Engineering, Imam Alkadhim University College, Baghdad, Iraq

Email: mokhalad.khaleel@iku.edu.iq

## Abstract

*The advancement of pressure sensors customized for purposes marks notable progress, in healthcare diagnostics and patient supervision. This article delves into creating and assessing of a capacitive pressure sensor designed to measure physiological pressures with utmost accuracy and sensitivity. The sensor's structure integrates materials compatible with the body to ensure safety and dependability when interacting with bodily tissues. Thorough simulations and validations showcase the sensors performance emphasizing its responsiveness across various pressures in medical settings. The assessment encompasses an analysis of the sensor's sensitivity at (12.4 fF/mmHg) exceptional linearity within a nonlinearity range of  $\pm 0.015\%$  with a small diaphragm diameter (0.5 mm) and long-term reliability. The results indicate that the suggested capacitive pressure sensor exhibits promising possibilities for use in fields like blood pressure monitoring, intracranial pressure measurement and other crucial areas of biomedicine, providing a nonintrusive and cost-efficient method, for real-time health monitoring and diagnostic purposes.*

## Keywords

**MEMS, Capacitive Pressure Sensor, Biomedical Application, Heart Diseases.**

## I. INTRODUCTION

Hypertension is an illness globally significantly increasing the risk of various conditions, like heart, brain and kidney issues [1–4]. Over the thirty years around 1.28 billion individuals between the ages of 30 and 79 have been diagnosed with hypertension. Only 14% have managed to keep it in check [5]. Studies suggest that closely tracking blood pressure variations over a day can help evaluate the effectiveness of medications and prevent heart diseases [6]. Consequently, there is a growing need, for blood pressure monitoring to promote well-being. Incorporation cutting-edge sensor technologies, into

the sector has greatly improved the effectiveness of healthcare diagnostics and patient monitoring systems [7–9]. Capacitive pressure sensors have become a choice because of their sensitivity, energy efficiency and ability to work with biocompatible materials [10, 11]. These sensors are especially useful in scenarios requiring pressure monitoring, such as blood pressure intracranial pressure and respiratory function [12, 13] as shown in Fig. 1.

Lately there has been a growing need, for monitoring systems that are noninvasive dependable and provide real-time data, this demand has led to advancements in pressure sensor technology [14]. Capacitive pressure sensors work by mea-



This is an open-access article under the terms of the Creative Commons Attribution License, which permits use, distribution, and reproduction in any medium, provided the original work is properly cited.  
©2026 The Authors.

Published by Iraqi Journal for Electrical and Electronic Engineering | College of Engineering, University of Basrah.

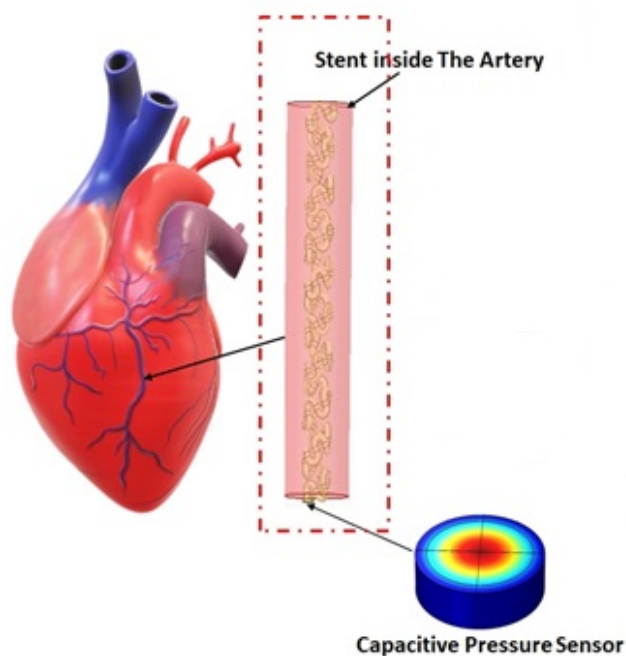


Fig. 1. Capacitance pressure sensor interacting with bodily tissues

suring changes in capacitance caused by pressure application offering a compact solution [15]. These sensors are particularly useful in fields where detecting even the smallest changes in pressure levels can signal health conditions. The different designs of MEMS sensors emphasized the size, sensitivity and materials utilized. Zawawi et al. utilized a 3C-SiC diaphragm measuring  $1.0 \times 1.0 \text{ mm}^2$  with a sensitivity to detect poisonous gases, though specific sensitivity values are not provided [16]. Sedaghat et al. implemented an aluminum square perforated diaphragm of  $0.5 \times 0.5 \text{ mm}^2$ , achieving an open circuit sensitivity of  $6.677 \text{ mV/Pa}$ , demonstrating a moderate sensitivity level [17]. Nicollini et al. used a poly-Si rectangular diaphragm ( $0.5 \times 1.0 \text{ mm}$ ) with a significant sensitivity of  $12.58 \text{ mV/Pa}$ , highlighting the efficacy of CMOS fabrication methods for achieving high sensitivity [18]. Ganji et al. employed a smaller silicon square perforated diaphragm ( $0.3 \times 0.3 \text{ mm}^2$ ), which showed an open circuit sensitivity of  $2.46 \text{ mV/Pa}$ , indicating lower sensitivity than larger diaphragms [19]. Jantawong et al. and Mustapha et al. used circular flat diaphragms with  $930 \text{ }\mu\text{m}$  and  $40 \text{ }\mu\text{m}$  diameters, respectively [20,21]. Mustapha's graphene diaphragm demonstrated extremely low sensitivity at  $0.035 \text{ mV/Pa}$ , suggesting limitations in miniaturized graphene-based sensors. Auliya et al. utilized a Si/SiC/tungsten corrugated diaphragm with a

$2.0 \text{ mm}$  diameter, achieving a sensitivity of  $0.15 \text{ mV/Pa}$  [22], which, while higher than Mustapha's design, still reflects moderate sensitivity levels for larger diaphragms. Malik et al. focused on hearing aids, using a Si<sub>3</sub>N<sub>4</sub> diaphragm with an area of  $7850 \text{ }\mu\text{m}^2$ , achieving an open circuit sensitivity of  $0.086 \text{ mV/Pa}$ , suitable for audio applications [23]. Wood et al. used a larger graphene/PMCMir diaphragm with a  $3.5 \text{ mm}$  diameter, demonstrating a sensitivity of  $10 \text{ mV/Pa}$  [24], indicative of the high potential of larger diaphragms in achieving superior sensitivity. This paper presents the design and analysis of a small capacitive pressure sensor with diameter  $0.5 \text{ mm}$ , optimized for biomedical applications and using biocompatible material. The proposed sensor incorporates advanced techniques regarding to small diaphragm size and biocompatible materials to ensure safe and effective integration with human tissues. The design process includes the selection of suitable materials, and geometric optimization.

## II. METHODOLOGY

The design and analysis of the capacitive pressure sensor with a circular shape for biomedical applications were carried out using COMSOL Multiphysics software. The process began with the geometric design of the sensor, where key parameters such as the diameter, thickness of the dielectric layer, and electrode spacing were determined to ensure optimal performance and uniform pressure distribution as shown in Table I.

TABLE I.  
ILLUSTRATE THE DETAILS OF THE CAPACITIVE PRESSURE DESIGN

Parameters	Units
Diameter of Sensor	0.5 mm
Substrate thickness	20 $\mu\text{m}$
Bottom electrode thickness	500 nm
Top electrode thickness	500 nm
Dielectric layer thickness	3 $\mu\text{m}$

Biocompatible materials, including gold for the electrodes and Titanium Dioxide (TiO<sub>2</sub>) for the dielectric layer which has a very high dielectric constant, biocompatible, chemical stability, and mechanical Strength were selected to ensure safety and compatibility with human tissues as shown in Table II.

A comprehensive 3D model of the sensor was then created in COMSOL Multiphysics as shown in figure 2. This model included precise definitions of geometry and material properties, along with appropriate boundary conditions to simulate the application of pressure on the sensor surface. The model was discretized using a fine mesh to ensure high accuracy in the simulation results, particularly in areas with significant

TABLE II. ILLUSTRATE MATERIAL TYPES FOR ALL PARTS OF THE SENSOR

Parameters	Material
Substrate	Polyamide
Anchor	Polyamide
Electrode	Gold
Dielectric Layer	Titanium Dioxide

electric field gradients and mechanical stress.

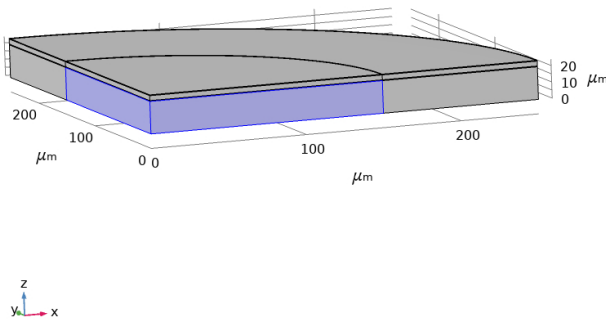


Fig. 2. 3D structure of capacitance pressure sensor

The sensor typically consists of one plate and a diaphragm. One plate is usually fixed, while the diaphragm is flexible and moves under pressure. Dielectric material is placed between the diaphragm and plate. This material serves to provide insulation, influencing the overall capacitance. In the absence of applied pressure, the sensor has a baseline capacitance determined by the area of the plates, the distance between the plates and the dielectric material based on equation 1. Since capacitance is inversely proportional to the distance between the diaphragm and plate, so when external pressure is applied, it causes the flexible diaphragm to move and reduces the distance between the plates, causing the capacitance to increase. The change in the separation distance directly alters the capacitance of the system. The higher of the applied pressure leads to increase the deformation of the diaphragm, then a larger change in capacitance. The tests used the electrostatics and solid mechanics components in COMSOL to assess the sensors effectiveness. The electrostatics component measured variations, in capacitance caused by pressure while the solid mechanics component analyzed how the sensor deformed mechanically. Several tests were performed at pressure levels to

collect information, on capacitance values linked to pressure levels. The equation defines the capacitance (C):

$$C = \frac{\epsilon_r \epsilon_0 A}{d} \quad (1)$$

where: ( $\epsilon_r$ ) is the relative permittivity of the dielectric material, ( $\epsilon_0$ ) is the vacuum permittivity  $8.854 \times 10^{-12}$  F/m, A is the area of the capacitor plates, and d is the separation between the plates. The sensitivity and linearity of the sensor were calculated from the simulation data. Sensitivity, defined as the change in capacitance per unit pressure, was determined by plotting capacitance versus applied pressure and calculating the slope of the resulting curve:

$$S = \frac{\Delta C}{\Delta P} \quad (2)$$

To change in the gap  $\Delta d$  with pressure must be considered to estimate sensitivity. Assuming the pressure causes a small deformation in the dielectric material, the change in gap  $\Delta d$  is related to the applied pressure (P) using Hooke's Law:

$$\Delta d = \frac{P \cdot d}{E} \quad (3)$$

where: P is the applied pressure, d is the initial thickness of the dielectric layer, and E is the Young's modulus of the dielectric layer. The change in capacitance  $\Delta C$  due to deformation  $\Delta d$  is calculated as:

$$\Delta C = \frac{\epsilon_r \epsilon_0 A \Delta d}{d^2} \quad (4)$$

The researchers assessed linearity using a regression model to analyze the capacitance pressure data. They calculated the coefficient of determination ( $R^2$ ) to measure linearly how the sensor's readings aligned with the applied pressure. The formula, for the linear regression model is as follows;

$$C_{fit} = b + mP \quad (5)$$

The difference, from the straight-line approximation is computed as;

$$\Delta C = C_{measure} - C_{fit} \quad (6)$$

The full-scale output (FSO) refers to the variance in capacitance corresponding to the lowest pressure levels.

$$FSO = C_{max} - C_{min} \quad (7)$$

The nonlinearity percentage is calculated as:

$$\text{Nonlinearity}\% = \left( \frac{\Delta C_{max}}{FSO} \right) \times 100 \quad (8)$$

The methodology ended by discussing how well the sensor performs looking at its sensitivity and linearity and assessing whether it is suitable, for use in settings. The study seeks to show how effective the sensor is in measuring pressure for diagnosis and monitoring patients laying the groundwork for further research and advancement, in this area.

### III. RESULTS AND DISCUSSION

The development and evaluation of the pressure sensor, revealed several important discoveries. The findings from the COMSOL simulations are thoroughly examined to evaluate the sensors effectiveness, such as its sensitivity, linearity and overall dependability. In Fig. 3 there is a representation of a simulation demonstrating displacement when pressure is applied to a circular sensor. The graph illustrates how strain is distributed across the sensor providing insights into its response, to pressure. Figure 4 shows how a MEMS capacitive

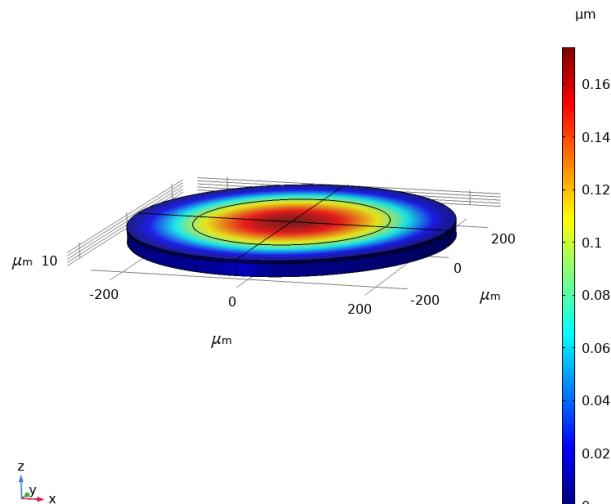


Fig. 3. Illustrates the 3D simulation showing how an object moves in reaction to pressure being applied

pressure sensor reacts, to pressures ( $P_0$ ) from 0 to 30 kPa. The displacement refers to the physical movement of one of a diaphragm in response to applied pressure, which it is measured in micrometers ( $\mu\text{m}$ ) increases linearly with the applied pressure starting at around  $0.01 \mu\text{m}$  at 0 kPa and reaching  $0.17 \mu\text{m}$  at 30 kPa. This linear relationship indicates that the sensor behaves consistently and predictably which is crucial for pressure readings. The clustered data points on the line demonstrate the sensors precision and repeatability. These qualities are essential for pressure monitoring applications, such as medical diagnostics and industrial automation. The clear labeling of axes and consistent use of markers make it

easier to understand the plot. This thorough analysis highlights how well the sensor design delivers a displacement response to pressure levels confirming its suitability, for high precision tasks. Fig. 5 in the presentation shows how capaci-

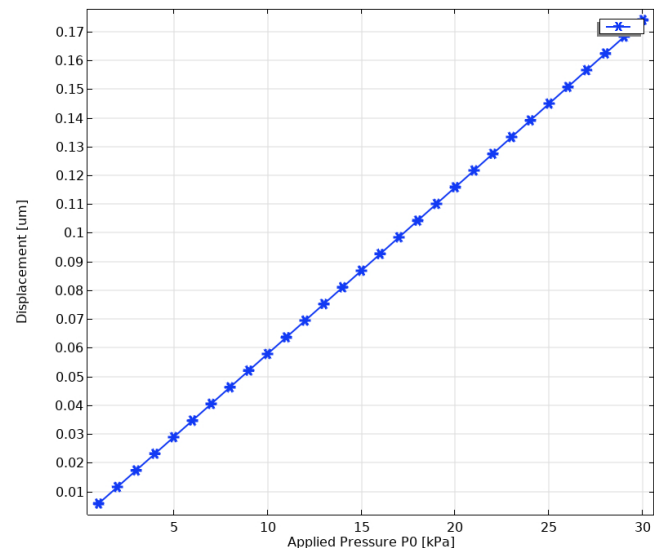


Fig. 4. Shows how a MEMS capacitive pressure sensor reacts when different pressures are applied

tance changes with pressure for a pressure sensor. The data indicates a relationship with capacitance values ranging from around  $46.4 \text{ pF}$  to  $49.2 \text{ pF}$  as pressure increases from 0 to 30 kPa based on equation 4. This linear pattern highlights the sensors sensitivity and accuracy from the grouped data points aligning well with the straight line. The consistency suggests that the sensor is reliable in measuring pressure changes. The clear labeling of axes (capacitance in picofarads and pressure intensity in kilopascals) makes it easy to understand the data. Using star markers and connecting lines improves visibility, emphasising the sensor's calibration accuracy. This connection is crucial for applications that require pressure monitoring, such as industrial settings where knowing how the sensor responds to pressure changes is vital, for accurate readings based on capacitance values. The capacitive pressure sensor created for use shows a level of sensitivity. With a  $92 \text{ fF/bar}$  sensitivity, it can accurately detect the pressure changes, which is essential, for monitoring subtle fluctuations in the human body. This sensor design utilizes materials and unique structural setups to achieve precision ensuring reliable performance in demanding medical scenarios. High sensitivity improves capabilities and leads to better patient outcomes by enabling more precise and timely medical interventions. Fig. 6 shows how changes with applied pressure ( $P_0$ ) for pressure sensors with varying diaphragm thicknesses (dte). The graph covers a pressure range from 0 to 30 kPa. Shows the resulting

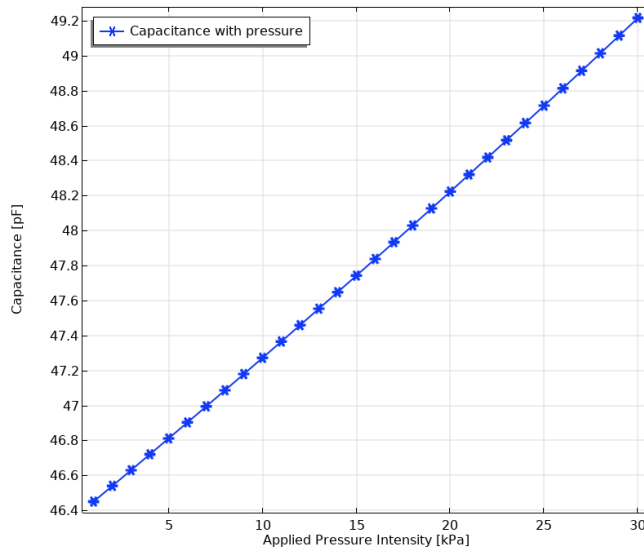


Fig. 5. Show capacitance changes with levels of pressure applied

displacement in micrometers ( $\mu\text{m}$ ) based on equation 3. Each line on the graph represents a diaphragm thickness ranging from  $0.5 \mu\text{m}$  to  $4.5 \mu\text{m}$ . The linear relationship observed in each case indicates that displacement increases proportionally with applied pressure with the slope of each line changing based on diaphragm thickness. Thinner diaphragms display displacement for a given pressure due to their increased sensitivity while thicker diaphragms exhibit reduced displacement indicating stiffness. The data points are closely grouped. Consistently align, with their respective trend lines showcasing the accuracy and consistency of the measurements. This thorough examination of displacement versus pressure for diaphragm thicknesses is essential for improving sensor design guaranteeing pressure readings in various working conditions and applications. The distinct labeling and color-coded markers for each diaphragm thickness improve the clarity and understanding of the graph turning it into a resource, for scientists and engineers involved in pressure sensor advancements. The graph in Fig. 7 illustrates how capacitance changes with pressure levels for pressure sensors with varying diaphragm thicknesses ranging from  $0.5 \mu\text{m}$  to  $4.5 \mu\text{m}$ . The pressure ranges from 0 to 30 kPa. Capacitance is measured in picofarads (pF). Each line on the graph represents a diaphragm thickness that shows a linear increase in capacitance as pressure increases. Thinner diaphragms, like the  $0.5 \mu\text{m}$  one display changes in capacitance indicating a sensitivity to pressure variations. On the other hand, thicker diaphragms such as the  $4.5 \mu\text{m}$  exhibit changes in capacitance suggesting lower sensitivity but potentially increased durability. The consistent arrangement of data points on each line implies repeatable sensor measurements.

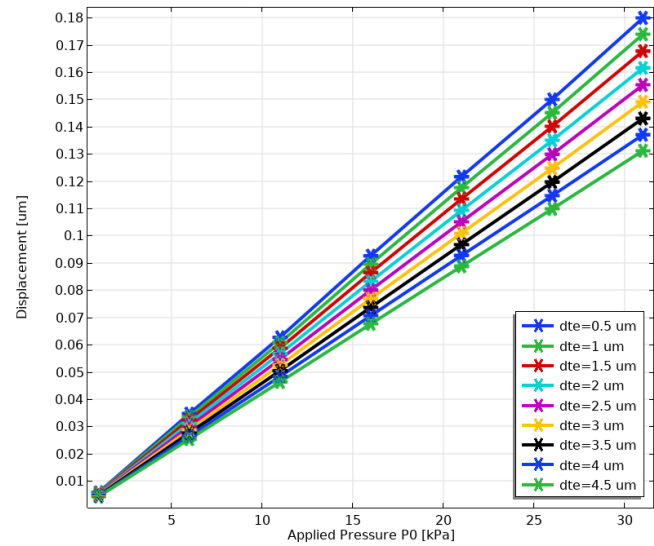


Fig. 6. Illustrates how the displacement of capacitive pressure sensors changes based on the thickness of the diaphragm

Using colors and markers, for each diaphragm thickness enhances the clarity and understanding of the plot. This detailed analysis provides critical insights for optimizing diaphragm thickness in capacitive pressure sensors, balancing sensitivity and durability to meet specific application requirements. Such data is essential for developing high-performance sensors for various industrial, medical, and environmental monitoring applications.

Figure 7 presents the nonlinearity characteristics of a MEMS capacitive pressure sensor, plotted as a function of applied pressure, ranging from 0 to 30 kPa. Nonlinearity, expressed as a percentage, is a critical parameter indicating the deviation from an ideal linear response. The plot reveals that the sensor's nonlinearity fluctuates across the pressure range. At 0 kPa, the nonlinearity is slightly negative, around  $-0.005\%$ . As pressure increases to 10 kPa, nonlinearity peaks at approximately  $0.01\%$ , indicating a positive deviation. However, at 20 kPa, the nonlinearity dips to its minimum, around  $-0.01\%$ , before rising again to  $0.005\%$  at 30 kPa.

The excellent sensitivity and accuracy of the crafted capacitive pressure sensor, as shown in Table III, allow it to be used in medical settings, such as monitoring blood pressure, measuring intracranial pressure, and assessing respiratory function. This sensor's capacity to deliver immediate pressure data can greatly improve treatment and diagnostic options. Additionally, the non-intrusive design of the sensor provides a secure monitoring alternative for patients.

TABLE III. ILLUSTRATE THE VALIDATION RESULT WITH OTHER WORK DONE BY RESEARCHERS

Ref.	Year	Sensor Shape	Material	Dimension	Pressure Range (mmHg)	Sensitivity (fF/mmHg)
[25]	2014	Square	Silicon, Aluminum	(1.2 × 1.4 × 0.5) mm	-	5
[14]	2020	Square	Silicon, Aluminum, Silicon nitride	(300 × 300 × 74) μm	0-225	4.3
[8]	2022	Circular	Polyamide, Gold, Silicon Nitrite	Diameter (0.564) mm Thickness (1080.2) μm	0-240	9.94
Prop.		Circular	Polyamide, Gold, Titanium Dioxide	Diameter (0.5) mm Thickness (24) μm	0-225	12.4

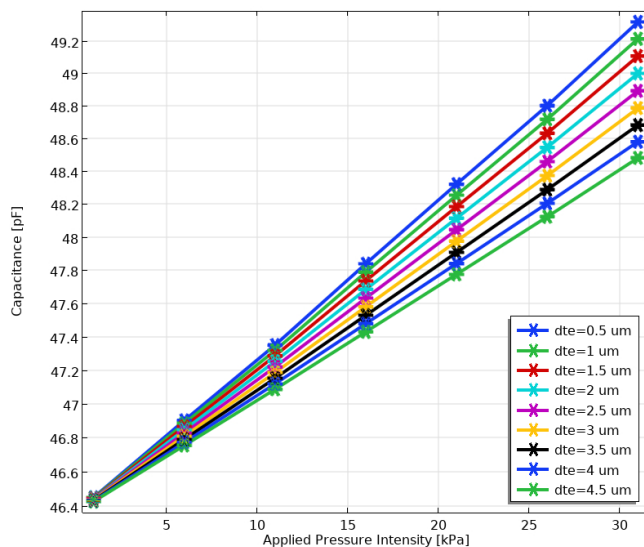


Fig. 7. The variation of capacitance for capacitive pressure sensors with different diaphragm thicknesses

#### IV. CONCLUSION

In summary, the capacitive pressure sensor created by using biocompatible material and evaluated in this research demonstrated high sensitivity at (12.4 fF/mmHg), exceptional linearity within a nonlinearity range of  $\pm 0.015\%$ , and consistent performance proving its suitability for a range (0-225) mmHg. The positive verification of the sensor, via simulations and real-world trials, highlights its promise in improving healthcare diagnostics and patient supervision. Ongoing efforts will concentrate on refining the sensors' structure and broadening its range of applications to advance technology and enhance well-being.

#### CONFLICT OF INTEREST

The authors have no relevant conflict of interest to this article.

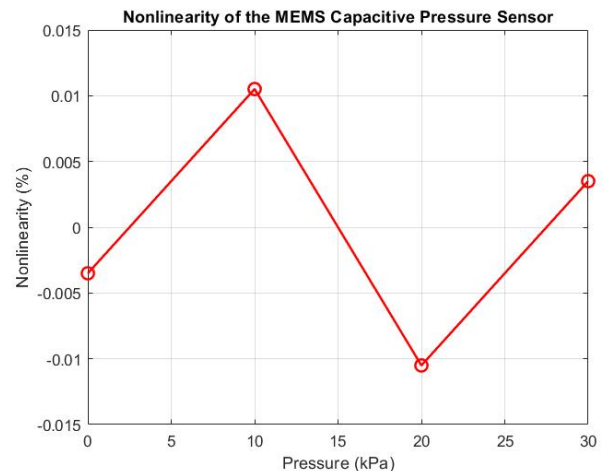


Fig. 8. Nonlinearity characteristics of the MEMS capacitive pressure sensor across applied pressure range from 0 to 30 kPa

#### REFERENCES

- [1] L.-Y. Ma, W.-W. Chen, R.-L. Gao, L.-S. Liu, M.-L. Zhu, Y.-J. Wang, Z.-S. Wu, H.-J. Li, D.-F. Gu, Y.-J. Yang, et al., "China cardiovascular diseases report 2018: an updated summary," *Journal of geriatric cardiology: JGC*, vol. 17, no. 1, p. 1, 2020.
- [2] S. Liu, Y. Li, X. Zeng, H. Wang, P. Yin, L. Wang, Y. Liu, J. Liu, J. Qi, S. Ran, et al., "Burden of cardiovascular diseases in china, 1990-2016: findings from the 2016 global burden of disease study," *JAMA cardiology*, vol. 4, no. 4, pp. 342–352, 2019.
- [3] C. A. T. Radovanovic, L. A. d. Santos, M. D. d. B. Carvalho, and S. S. Marcon, "Arterial hypertension and other risk factors associated with cardiovascular diseases among adults," *Revista latino-americana de enfermagem*, vol. 22, no. 4, pp. 547–553, 2014.
- [4] S. Allender, P. Scarborough, V. Peto, M. Rayner, J. Leal, R. Luengo-Fernandez, and A. Gray, "European cardio-

- vascular disease statistics,” *European Heart Network*, vol. 3, pp. 11–35, 2008.
- [5] B. Zhou, R. M. Carrillo-Larco, G. Danaei, L. M. Riley, C. J. Paciorek, G. A. Stevens, E. W. Gregg, J. E. Bennett, B. Solomon, R. K. Singleton, et al., “Worldwide trends in hypertension prevalence and progress in treatment and control from 1990 to 2019: a pooled analysis of 1201 population-representative studies with 104 million participants,” *The Lancet*, vol. 398, no. 10304, pp. 957–980, 2021.
- [6] M. Alghrairi, N. Sulaiman, and S. Mutashar, “Health care monitoring and treatment for coronary artery diseases: challenges and issues,” *Sensors*, vol. 20, no. 15, p. 4303, 2020.
- [7] G. S. Lakshmi, K. S. Rao, K. Guha, and K. G. Sravani, “Design of piezoresistive-based microcantilever for mems pressure sensor in continuous glucose monitoring system,” *Micro and Nanoelectronics Devices, Circuits and Systems: Select Proceedings of MNDCS 2021*, pp. 371–379, 2022.
- [8] M. Alghrairi, N. Sulaiman, W. Z. W. Hasan, H. Jaafar, and S. Mutashar, “Design a wireless pressure sensor with an ellipse and a circular shape to monitor the pressure within the coronary artery,” *IEEE Access*, vol. 10, pp. 92158–92165, 2022.
- [9] M. Alghrairi, N. Sulaiman, W. Z. W. Hasan, H. Jaafar, and S. Mutashar, “Analysis of four coils by inductive powering links for powering bio-implantable sensor,” *TEM Journal*, vol. 11, no. 3, 2022.
- [10] K. Jagabathuni and S. Peravali, “Analysis on various clamping models of square shaped diaphragm in capacitive pressure sensor for intra ocular pressures,” in *2022 International Conference on Computing, Communication, and Intelligent Systems (ICCCIS)*, pp. 1–6, IEEE, 2022.
- [11] V. S. Kulkarni and S. S. Chorage, “An efficient mems sensor modelling by geometrical parameter optimization,” *International Journal of Electronics and Telecommunications*, pp. 287–291, 2022.
- [12] S. A. Zawawi, A. A. Hamzah, B. Y. Majlis, and F. Mohd-Yasin, “A review of mems capacitive microphones,” *Micro machines*, vol. 11, no. 5, p. 484, 2020.
- [13] M. Alghrairi, N. Sulaiman, S. Mutashar, W. Z. Wan Hasan, H. Jaafar, and W. Algriree, “Designing and analyzing multi-coil multi-layers for wireless power transmission in stent restenosis coronary artery,” *AIP Advances*, vol. 12, no. 12, 2022.
- [14] K. S. Rao, W. Samyuktha, D. V. Vardhan, B. G. Naidu, P. A. Kumar, K. G. Sravani, and K. Guha, “Design and sensitivity analysis of capacitive mems pressure sensor for blood pressure measurement,” *Microsystem Technologies*, vol. 26, no. 8, pp. 2371–2379, 2020.
- [15] M. Xu, Y. Feng, X. Han, X. Ke, G. Li, Y. Zeng, H. Yan, and D. Li, “Design and fabrication of an absolute pressure mems capacitance vacuum sensor based on silicon bonding technology,” *Vacuum*, vol. 186, p. 110065, 2021.
- [16] S. Zawawi, A. Hamzah, F. Mohd-Yasin, and B. Majlis, “Mechanical performance of sic based mems capacitive microphone for ultrasonic detection in harsh environment,” in *Nanoengineering: Fabrication, Properties, Optics, and Devices XIV*, vol. 10354, pp. 211–217, SPIE, 2017.
- [17] S. B. Sedaghat and B. A. Ganji, “A novel mems capacitive microphone using spring-type diaphragm,” *Microsystem Technologies*, vol. 25, pp. 217–224, 2019.
- [18] G. Nicollini and D. Devecchi, “Mems capacitive microphones: Acoustical, electrical, and hidden thermal-related issues,” *IEEE Sensors Journal*, vol. 18, no. 13, pp. 5386–5394, 2018.
- [19] B. A. Ganji, S. B. Sedaghat, A. Roncaglia, and L. Belsito, “Design and fabrication of very small mems microphone with silicon diaphragm supported by z-shape arms using soi wafer,” *Solid-State Electronics*, vol. 148, pp. 27–34, 2018.
- [20] H. M. Mustapha, M. Wee, A. Zain, and M. A. Mohamed, “Characterization of graphene based capacitive microphone,” *Sains Malaysiana*, vol. 48, no. 6, pp. 1201–1207, 2019.
- [21] J. Jantawong, N. Atthi, C. Leepattarapongpan, A. Srisuwan, W. Jeamsaksiri, K. Sooriakumar, A. Austin, and S. Niemcharoen, “Fabrication of mems-based capacitive silicon microphone structure with staircase contour cavity using multi-film thickness mask,” *Microelectronic Engineering*, vol. 206, pp. 17–24, 2019.
- [22] R. Z. Auliya, M. R. Buyong, B. Yeop Majlis, M. F. Mohd. Razip Wee, and P. C. Ooi, “Characterization of embedded membrane in corrugated silicon microphones for high-frequency resonance applications,” *Microelectronics International*, vol. 36, no. 4, pp. 137–142, 2019.

- [23] S. Mallik, D. Chowdhury, and M. Chttopadhyay, "Development and performance analysis of a low-cost mems microphone-based hearing aid with three different audio amplifiers," *Innovations in Systems and Software Engineering*, vol. 15, pp. 17–25, 2019.
- [24] G. S. Wood, A. Torin, A. K. Al-mashaal, L. S. Smith, E. Mastropaolo, M. J. Newton, and R. Cheung, "Design and characterization of a micro-fabricated graphene-based mems microphone," *IEEE Sensors Journal*, vol. 19, no. 17, pp. 7234–7242, 2019.
- [25] M. Luo, A. W. Martinez, C. Song, F. Herrault, and M. G. Allen, "A microfabricated wireless rf pressure sensor made completely of biodegradable materials," *Journal of microelectromechanical systems*, vol. 23, no. 1, pp. 4–13, 2013.